Joint Optimization for Mobile Crowdsensing Systems with Reliability Consideration

Jiahui Feng, Yaru Fu, Zheng Shi, Yalin Liu, and Kevin Hung

***Abstract*—Mobile crowdsensing (MCS) uses sensor-embedded mobile devices to collect and share data. However, the unstable wireless channels and limited network resources deteriorate the reliability of data transmission in MCS networks. To tackle this issue, we propose a hybrid automatic repeat request (HARQ)-aided MCS framework in this paper. Within the framework, we formulate a reward maximization problem by jointly optimizing user selection, sensing data allocation, transmit power, and rate allocation, taking into account various practical constraints and outage requirement. To address the non-convexity of the formulated problem, we begin by transforming it into a long term average throughput (LTAT) maximization problem per user, assuming that all users would have the opportunity to participate in the sensing task. Nevertheless, solving the transformed problem remains challenging due to the intricate nature of the outage probability, which arises from the inherent coupling between transmission power and rate variables. To facilitate the analysis, a divide-then-conquer method is proposed. Specifically, we decompose the LTAT optimization problem into two subproblems: transmission power allocation and rate selection. To tackle the transmission power allocation subproblem, we reveal that the outage probability is convex with respect to transmission power. This inspires us to solve the non-convex power allocation subproblem by using an alternating iteration algorithm in conjunction with Dinkelbach's algorithm. Similar approach can be applied to rate selection. After resolving the two subproblems, an alternating optimization method is used to optimize transmission power and rate iteratively until convergence is achieved. At last, the user selection process is determined by selecting the users with the highest-ranked achievable rewards. Extensive simulation results verify the superiority of our proposed algorithm compared to various benchmark schemes.**

***Index Terms*—HARQ, mobile crowdsensing, reliability assurance, reward maximization, user selection.**

I. Introduction

THE rapid progress of Internet of Things (IoT) applications within smart city environments has facilitated a wide range of services [1], including smart transportation [2], pollution evaluation, traffic management [3], and public safety monitoring [4], among others. However, these services typically require a significant amount of data, which presents a challenge for conventional wireless sensor networks due to their limited sensing coverage and scalability [5]. To overcome this limitation, mobile crowdsensing (MCS) has emerged in recent years [6]. MCS leverages human-carried devices such as smartphones and smartwatches to sense and collect data [7], offering a promising solution to address the data collection bottleneck. In an MCS system, multiple mobile users serve as sensing service providers, while an agent platform is responsible for managing sensing tasks [8], [9]. When a specific sensing task is initiated, the agent identifies a suitable set of participating devices based on the task requirements. These selected devices then sense the environment, collect data, and transmit the collected data to the agent or server for further data processing [10]. Although MCS systems present significant advantages over traditional sensing architectures, they encounter some challenges when deployed in wireless edge networks. One such challenge is the potential failure of sensing data transmission due to limited communication resources, such as restricted wireless bandwidth and energy resources, as well as unstable wireless channels. To optimize the performance of MCS systems in resource-constrained networks, it becomes crucial to effectively leverage the available network resources and device resources. Therefore, special attention must be drawn to the co-design of sensing and transmission components within the MCS system. By considering and optimizing both aspects, the overall performance and efficiency of the MCS system can be significantly enhanced.

A. Literature Review

In this section, we provide a comprehensive review of the existing research on user selection/task allocation, data sensing, and transmission within MCS networks. Since the performance of the sensing task relies heavily on the appropriate assignment of tasks to mobile users, the participant selection (or task allocation) has been extensively investigated in the literature [11]–[15]. Specifically, in [11], the authors addressed the problem of dynamically selecting users by proposing both offline and online algorithms. They focused on a dynamic user selection problem with heterogeneous sensing tasks, with the goal of minimizing sensing costs while satisfying probabilistic coverage constraints. The authors of [12] selected the participants by considering the spatial distance between candidates and tasks, user willingness, and remaining battery of devices. In [13], the authors proposed an incentive framework, that is, user selection depended on the user's quality of information or high-quality data. The authors in [14] focused on a duration-sensitive task allocation model. The objective of the model was

This work was supported in part by the grant from the Research Grants Council (RGC) of the Hong Kong Special Administrative Region, China under Reference No. UGC/FDS16/E02/22, in part by the Research Matching Grant (RMG) under Reference No. CP/2022/2.1, in part by the Team-based Research Fund under Reference No. TBRF/2024/1.10, in part by National Natural Science Foundation of China under Grant 62171200, and in part by Guangdong Basic and Applied Basic Research Foundation under Grant 2023A1515010900. (*Corresponding Author: Yaru Fu.*)

J. Feng, Y. Fu, Y. Liu and K. Hung are with the School of Science and Technology, Hong Kong Metropolitan University, Hong Kong, 999077, China (e-mail: s1365639@live.hkmu.edu.hk, yfu@hkmu.edu.hk, ylliu@hkmu.edu.hk, khung@hkmu.edu.hk).

Z. Shi is with the School of Intelligent Systems Science and Engineering, Jinan University, Zhuhai 519070, China (e-mail: zhengshi@jnu.edu.cn).

to maximize the number of completed tasks while considering the constraints of sensing duration and task capacity for each worker. In [15], an edge computing-based photo crowdsourcing framework was designed for 3D model reconstruction, where a set of photos was selected based on the target coverage requirement. Once the set of participants is determined in an MCS system, the sensing [16], [17] and transmission processes become essential areas of study [18]–[20]. More precisely, in [16], Xu *et al.* focused on data sensing design. Specifically, they proposed a vehicular crowdsensing system to design the sensing distribution of the sampled data to align with the desired target distribution according to the trajectories of mobile users. Similarly, the authors of [17] proposed a payment mechanism to guide the data sensing process. Particularly, they studied workers' strategic behavior, and motivate workers to provide high quality data. Moreover, the authors of [18] and [19] took into consideration the processes of data sensing and transmission in multi-task allocation schemes. These processes were simplified by assuming that the required data can always be successfully sensed and transmitted by each participant. However, a notable distinction is that [19] specifically ensured the sensing quality of individual tasks, providing an additional level of guarantee. [20] focused on the design of joint sensing and transmission rates control for energy efficient mobile crowd sensing in a given time duration.

Recently, the significance of jointly optimizing user selection, data sensing, and transmission in the design of MCS systems has been recognized. For example, in [21], the authors proposed a wireless powered crowdsensing framework that integrates power transfer, data sensing, compression, and transmission to maximize the operator's reward, wherein both the lossless compression and lossy compression are considered. Different from [21], the authors of [22] did not consider the data compression phase as they focused on the data sensing and transmission phase, and designed a unified framework. This framework jointly optimized the processes of user selection, bandwidth allocation, data sensing, and transmission to enhance the overall performance of MCS system. Nevertheless, [21] and [22] ignored the computation of sensed data and the impact of computation resource limitation. This research gap had been filled by [23], in which a cooperative data sensing and computation offloading scheme was proposed for the UAV-assisted MCS system with the aim of maximizing the overall system utility. The authors of [24] also addressed the computation phase in the MCS system. In [24], they developed a framework that integrates mobile sensing and computing, enabling the processing of sensed data locally on mobile devices. However, [23] and [24] overlooked the impact of sensed data transmission and the communication resource limitations. To conquer this issue, the authors in [25] proposed a joint sensing, computation, and transmission policy in multi-dimensional resource constrained MCS systems to maximize the total number of sensed bits for the task. Similar to [25], the data sensing, computation, and transmission were jointly investigated in [26], aiming to minimize the total completion time. Therein, the non-orthogonal multiple access (NOMA) technology was adopted to further reduce the total completion time. Although [23]–[26] involve a computational phase in MCS system, they do not consider the limitations of computing resources. [27] filled this research gap. In [27], they proposed a cooperative computing framework for MCS that leverages orthogonal frequency division multiple access based device-to-device links for task offloading. Although various studies [21]–[27] have addressed the data sensing, transmission, and even computation problems for MCS systems, it is important to acknowledge that existing works often oversimplify the data transmission process by assuming that transmitters know the accurate instantaneous channel state information (CSI). However, it is difficult for the transmitter to obtain accurate instantaneous CSI under fast fading channels due to the high overhead of channel estimation and feedback, or the long delay of channel estimation and feedback. So, this simplification does not align well with real requirements and can seriously affect the efficiency of resource allocation in MCS systems.

B. Our Contributions

Motivated by the aforementioned observations, this paper focuses on a hybrid automatic repeat request (HARQ)-aided MCS system for the joint design of user selection, data sensing, and communication. We consider a more realistic communication scenario in which transmitters rely on statistical CSI instead of instantaneous CSI. This realistic consideration can lead to data transmission failures. To ensure the reliability of data transmission, there are numerous techniques to enhance wireless transmission reliability, such as re-configurable intelligent surfaces (RIS) [28], unmanned aerial vehicle (UAV) [29], radio frequency relaying (RF) [30]. However, these technologies have certain limitation, as they require the transmitter to obtain the instantaneous CSI. In this paper, we explore the usage of HARQ as a solution. HARQ is an important technique for reliable transmission at the cost of increased latency. It can significantly enhance the reliability of the communication system when transmitters only know the statistical CSI. However, the application of HARQ also introduces inevitable delays to the MCS system. To mitigate the impact of HARQ-induced latency on the MCS system, a latency constraint has been incorporated in this study. Additionally, the HARQ protocol exhibits good compatibility and scalability, so it is widely used in various digital communication systems to ensure transmission reliability. In general, the HARQ techniques can be classified into three types based on the encoding and decoding operations at the transceivers, i.e., Type-I HARQ, HARQ with chase combining (HARQ-CC) and HARQ with incremental redundancy (HARQ-IR) [31]. In our work, we utilize all three types of HARQ schemes to ensure the reliability of MCS networks. For brevity, the main contributions of this paper are summarized as follows:

- A novel perspective on wireless transmission in MCS systems is introduced: the transmitter relies on statistical CSI rather than accurate instantaneous CSI. This realistic consideration can inevitably lead to data transmission failures within MCS systems. To address this issue, the three HARQ techniques are utilized to enhance transmission reliability.

- We design a joint sensing and imperfect communication framework in HARQ-aided MCS systems with constrained resources. In the framework, the processes of user selection, data sensing, transmission power, and rate allocation are jointly designed for maximizing the achievable reward of the system. Additionally, we takes into account the constraints imposed by task requirements, data transmission reliability, and resource limitations.
- The formulated optimization problem lacks explicit modality and a tractable form, and it is non-convex. Accordingly, it is difficult to solve efficiently by using conventional convex optimization techniques. Furthermore, the problem can not formulated as a problem of Markov decision process. Therefore, deep reinforcement learning schemes are not suitable for this problem. To address this issue, we develop an effective approach. Specifically, we first transform the system reward maximization problem into a long term average throughput (LTAT) maximization problem for each user by considering all users would have the opportunity to participate in the sensing task. However, the coupling of optimization variables, such as transmission power and rate significantly impacts the outage probability, making the task of solving the LTAT maximization problem more challenging. For simplicity, we divide the LTAT maximization problem into two subproblems, i.e., power allocation and rate selection.
- To solve the transmission power allocation subproblem, we show the convexity of outage probability with respect to transmission power. This allows us to solve the problem by combining alternatively iterating optimization and Dinkelbatch's algorithm. As far as the transmission rate optimization, a similar approach to the transmission power allocation subproblem can be applied to transform a non-convex fractional problem into a convex one. Afterwards, we utilize the alternating optimization method to optimize the two types of variables until convergence. Finally, the user selection process is determined by ranking users based on their achievable rewards and selecting the top-ranked users.
- Extensive numerical simulations are conducted to validate the effectiveness of our designed algorithms and the superiority of HARQ-IR technology.

The rest of this paper is organized as follows. Section II elaborates on the HARQ-aided MCS system model. In Section III, we formulate the problem of maximizing system's achievable reward by jointly optimizing data sensing and transmission. Section IV presents the proposed algorithm for the considered maximization problem. Simulation results as well as discussions are presented in Section V. At last, Section VI concludes this paper and highlights the future research directions. To enhance the readability of this work, the notations used throughout this paper are summarized in Table I.

TABLE I: List of Notations

Notation	Definition
$\mathcal{N}$	Index set of mobile users.
N	Total number of mobile users.
l_n	Participation decision of user n.
B	The number of subchannels.
z_n	Sensing data size of user n.
o_n	Sensing data rate of user n.
$t_{n,s}$	Sensing duration.
$E_{n,s}$	The energy consumed at the user n for data sensing.
e_n	Sensing energy consumption per bit.
$\mathcal{K}$	Index set of HARQ rounds.
K	The allowable maximum number of HARQ rounds.
$\mathbf{y}_{n,k}$	The received signal at the BS from user n in the k-th HARQ round.
$P_{n,k}$	The transmission power in the k-th HARQ round for user n.
$h_{n,k}$	Rayleigh channel coefficient for user n in k-th HARQ round.
$\mathbf{s}_{n,k}$	The sensing signal vector for user n in k-th HARQ round.
$\mathbf{w}_{n,k}$	The AWGN for user n in k-th HARQ round.
$\alpha^2_{n,k}$	The average channel power gain for user n in k-th HARQ round.
$\sigma^2_{n,k}$	The variance of AWGN for user n in k-th HARQ round.
$I_{n,k}$	The accumulated mutual information for user n in k-th HARQ round.
R_n	The transmission rate of user n.
$p_{\text{out},n,K}$	The outage probability after K HARQ rounds for user n.
$E_{n,c}$	The transmission energy consumption for user n.
Ψ	The total energy consumption.
$\bar{t}$	The average duration of each HARQ round for data transmission.
$\bar{P}_n$	The total average transmission power of user n.
$\mathcal{T}_n$	LTAT.
$t_{n,c}$	The data transmission duration.
$\mathcal{R}$	The reward.
$\boldsymbol{l}$	User selection policy.
$\boldsymbol{z}$	Sensing data size vector of all users.
$\boldsymbol{R}$	Transmission rate strategy.
$\boldsymbol{P}_n$	Transmit power vector of all HARQ rounds for user n.
$\boldsymbol{P}$	Transmit power vector of all users.

II. SYSTEM MODEL

As illustrated in Fig. 1, we consider a HARQ-aided MCS system, which consists of a base station (BS) and an edge server serving a group of N mobile users, whose index set is referred to as $\mathcal{N} = \{1, 2, \cdots, N\}$. Besides, a MCS agent is deployed at the server. In the proposed model, the mobile users periodically transmit their parameters, such as channel gain and available energy, to the MCS agent. Through these parameter updates, the agent is able to keep up-to-date information about the associated users' states. When a sensing task arrives, the agent utilizes the gathered information to make informed decisions. More specifically, based on the requirements of the sensing task and the current states of the users, the agent determines the user selection, data sensing allocation, and transmission policies. This selection process ensures that the most suitable user(s) are chosen and appropriate policies are applied for efficient and effective task execution. Therefore, the user selection strategy depends on user's performance, unlike the approaches in [32], [33]. Subsequently, the selected users complete their data sensing task and transmit the acquired data to the server. To ensure reliability during the transmission process, HARQ technique is employed. We take HARQ-IR as an example, and its protocol is depicted in Fig. 1 and operates as follows: in the initial HARQ round, the transmitter sends data 1. The receiver then attempts to decode data 1. If the receiver successfully decodes data 1, a positive acknowledgement (ACK) message is sent back to the transmitter and a new cycle of HARQ will be triggered. Otherwise, a negative acknowledgement (NACK) message will be fed back to the transmitter. The receiver stored the previously failed data packets and combined them with the subsequent data packet to decode.

A. User Selection and Data Sensing Model

For any user $n \in \mathcal{N}$, we introduce a binary variable, denoted as l_n for user n. This variable represents whether or not user

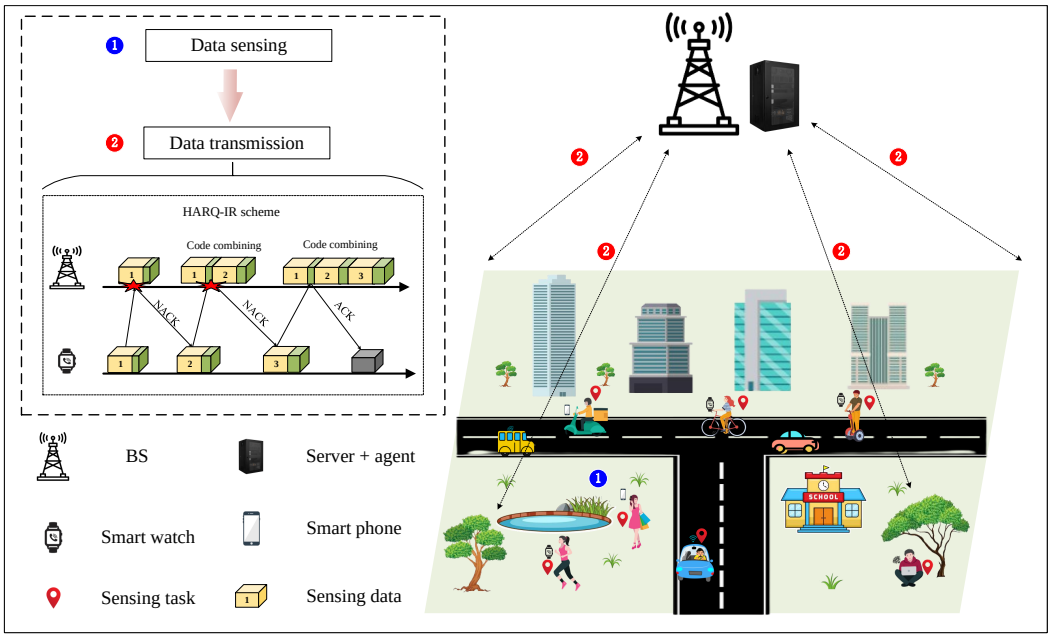

Fig. 1: An illustration of the HARQ-aided MCS systems.

n is selected for sensing the task. If and only if user n is selected, we have $l_n = 1$. Otherwise, $l_n = 0$. For the selected user, a subchannel is allocated to it for data transmission. In our system, we asume that all subchannels have a normalized bandwidth of one. Let B be the total available subchannels in the system, which indicates that a maximum of B users can be selected to participate in the sensing task. Therefore, we have the following constraint for all participate users as follows:

$$\sum_{n=1}^{N} l_n \leq B. \tag{1}$$

Once the user n is chosen to participate in a sensing task, the MCS agent will inform the user n regarding the size of sensing data, denoted as z_n. The relationship between z_n and user selection parameter l_n is $z_n(1-l_n) = 0$, which indicates $z_n = 0$ if l_n=0 and $z_n > 0$ if $l_n = 1$. Let o_n as the sensing data rate of user n, which is determined by the types of data to be sensed [22]. Given the sensing data size z_n, the sensing duration $t_{n,s}$ can be calculated as follows:

$$t_{n,s} = \frac{z_n}{o_n}. \tag{2}$$

Let $E_{n,s}$ be the energy consumed at the user n for data sensing, which can be expressed as follows:

$$E_{n,s} = e_n z_n, \tag{3}$$

where e_n is the sensing energy consumption per bit.

B. Data Transmission Model

In our work, we employ the HARQ technique to improve reception reliability in MCS systems. We assume that the allowable maximum number of HARQ rounds for each message is K, referred to as $\mathcal{K} = \{1, 2, \cdots, K\}$. Specifically, for $n \in \mathcal{N}$ and $k \in \mathcal{K}$, we consider the received signal at the BS from user n in the k-th HARQ round, which is expressed as follows:

$$\mathbf{y}_{n,k} = \sqrt{P_{n,k}} h_{n,k} \mathbf{s}_{n,k} + \mathbf{w}_{n,k}, \tag{4}$$

wherein $P_{n,k}$ denotes the transmission power in the k-th HARQ round for user n, $h_{n,k}$ is Rayleigh channel coefficient with average power of $\alpha_{n,k}^2$, i.e., $\mathbb{E}\{|h_{n,k}|\} = \alpha_{n,k}^2$, where $\mathbb{E}\{\cdot\}$ depicts the expectation operation. In addition, $\mathbf{s}_{n,k}$ represents the sensing signal vector in the k-th HARQ round for user n, and $\mathbf{w}_{n,k}$ represents the complex additive white Gaussian noise (AWGN) with zero mean and variance $\sigma_{n,k}^2$.

We discuss three types of HARQ schemes, namely, Type-I HARQ, HARQ-CC, and HARQ-IR [31]. Each of these schemes has different characteristics and principles for improving transmission reliability in the MCS system. Specifically, in Type-I HARQ, the receiver attempts to decode the message based solely on the currently received packet. If the packet is received correctly, it is successfully decoded and utilized. However, if the packet is received with errors, it will be discarded and not used for further decoding attempts. Meanwhile, with regard to HARQ-CC, the receiver stores the previously failed packets and combines them with the subsequent packet using maximum ratio combining (MRC) to improve the decoding performance. This allows for a more effective utilization of the received information. Regarding HARQ-IR, the previously failed packets are stored and combined with the subsequent packets that contain additional redundant information. This incremental redundancy allows for enhanced error correction capabilities and improved decoding performance at the cost of system complexity. From the information theoretical perspective [34], the expressions for the accumulated mutual information of the three HARQ

schemes differ, and they are quoted below:

$$I_{n,K} = \begin{cases} \max\limits_{k=1,\cdots,K} \log_2\left(1+\frac{P_{n,k}|h_{n,k}|^2}{\sigma_{n,k}^2}\right), & \text{Type-I} \\ \log_2\left(1+\sum\limits_{k=1}^{K}\frac{P_{n,k}|h_{n,k}|^2}{\sigma_{n,k}^2}\right), & \text{CC} \\ \sum\limits_{k=1}^{K}\log_2\left(1+\frac{P_{n,k}|h_{n,k}|^2}{\sigma_{n,k}^2}\right). & \text{IR} \end{cases} \tag{5}$$

To evaluate the transmission reliability of HARQ-aided M-CS system, the outage probability has been proved as the most fundamental performance metric of HARQ schemes. More precisely, the outage probability is defined as the probability of the event that the accumulated mutual information is less than the transmission rate R_n [35]. On this basis, the outage probability after K HARQ rounds for user n is given below:

$$p_{\text{out},n,K} = \Pr\left\{I_{n,K} < R_n\right\}. \tag{6}$$

Given the sensing data size z_n, let $E_{n,c}$ denote the transmission energy consumption, which is calculated by

$$\begin{aligned} E_{n,c} &= \mathbb{E}\left\{z_n \times \frac{\Psi}{z_n}\right\} \\ &= z_n \mathbb{E}\left\{\frac{\Psi}{z_n}\right\}, \end{aligned} \tag{7}$$

where Ψ denotes the total energy consumption. By utilizing the law of large numbers [36], (7) is rewritten as

$$\begin{aligned} E_{n,c} &= z_n \lim_{z_n\to\infty}\frac{\Psi}{z_n} \\ &= z_n \lim_{z_n\to\infty}\frac{\Psi}{Kt}\frac{1}{z_n/(Kt)}, \end{aligned} \tag{8}$$

where t represents the average duration of each HARQ round for data transmission. Since HARQ transmissions can be described as a renewal reward process, (8) can be derived based on the renewal-reward theorem as

$$E_{n,c} = z_n \frac{\mathbb{E}\left\{\frac{\Psi}{Kt}\right\}}{\mathbb{E}\left\{\frac{z_n}{Kt}\right\}}, \tag{9}$$

According to [34], [37], (9) is expressed as

$$E_{n,c} = z_n \frac{\bar{P}_n}{\mathcal{T}_n}. \tag{10}$$

where $\bar{P}_n = \mathbb{E}\left\{\Psi/(Kt)\right\} = \sum_{k=1}^{K} p_{\text{out},n,k-1} P_{n,k}$ denotes the total average transmission power of user n [38]. $\mathcal{T}_n = \mathbb{E}\left\{z_n/(Kt)\right\}$ represents the LTAT, which is measured in bits per second per hertz [37]. By using the above outage probability, the LTAT of three HARQ schemes can be mathematically expressed as:

$$\mathcal{T}_n = \frac{R_n\left(1-p_{\text{out},n,K}\right)}{\sum_{k=1}^{K} p_{\text{out},n,k-1}}. \tag{11}$$

Moreover, let $t_{n,c}$ as the data transmission duration. According to (12), $t_{n,c}$ is derived as

$$t_{n,c} = \frac{z_n}{\mathcal{T}_n}. \tag{12}$$

C. MCS Performance Metric

We utilize the reward of the agent as the performance metric. The reward represents the net utility obtained from the sensed data, taking into account the payments made to the individual users for their contribution to the sensing task [21], [22], [39], [40]. Mathematically, the reward, denoted as $\mathcal{R}$, can be expressed as follows:

$$\mathcal{R} = \sum_{n=1}^{N} U\left(z_n\right) - \sum_{n=1}^{N} M\left(z_n\right), \tag{13}$$

where $U\left(z_n\right)$ denotes the utility of z_n-bit sensed data contributed by user n, and $M\left(z_n\right)$ is the payment to user n based on the z_n-bit sensed data [22]. In our approach, we denote the utility of the sensed data delivered by user n utilising a commonly-used logarithmic function similar to [21], [22]. Specifically, we adopt the function $U\left(z_n\right) = c_n \log\left(1+z_n\right)$ to quantify the utility, where c_n is a weighting factor. This factor is introduced to account for the importance or significance of the specific type of data delivered by user n. It is noticed that the increasing monotonicity of the utility function indicates that having more information-rich data can enhance data utility, e.g., higher image/video resolution [41] and machine-learning accuracy [42]. Moreover, each selected user is paid based on the contribution made [22], [43], which is featured by its sensed data. As a result, the payment function is modeled as $M\left(z_n\right) = m_n \log\left(1+z_n\right)$, where m_n can be taken as a unit payment with respect to the unit data utility. Based on the foregoing discussions, the reward of agent is then simplified as below:

$$\mathcal{R} = \sum_{n=1}^{N} a_n \log\left(1+z_n\right). \tag{14}$$

where $a_n > 0$ and $a_n = c_n - m_n$.

III. Problem Formulation

In this paper, we focus on maximizing the reward of system through a joint optimization of several variables. These variables include the user selection policy, the sensing data size, the transmission rate, and the user transmission power of each HARQ round. Thereof, we take into account diversified constraints, including the delay requirement, energy limitation, average total transmission power constraint, data transmission quality constraint, the number of subchannels constraint, and the maximum transmission number of HARQ rounds. For notation simplicity, we denote by $\boldsymbol{l} = \left(l_n\right)_{n\in\mathcal{N}}$, $\boldsymbol{z} = \left(z_n\right)_{n\in\mathcal{N}}$ and $\boldsymbol{R} = \left(R_n\right)_{n\in\mathcal{N}}$ the user selection policy, the sensing data size vector of all users, and the transmission rate strategy, respectively. In addition, we define $\boldsymbol{P}_n = \left(P_{n,k}\right)_{k\in\mathcal{K}}$ and $\boldsymbol{P} = \left(\boldsymbol{P}_n\right)_{n\in\mathcal{N}}$ as the transmit power vector of all HARQ rounds for user n and the transmit power vector of all users, respectively. With these definitions, the maximization problem is mathematically formulated as follows:

$$\max_{\boldsymbol{l},\boldsymbol{z},\boldsymbol{R},\boldsymbol{P}} \quad \mathcal{R} \tag{15}$$

$$\text{s.t.} \quad \frac{z_n}{o_n} + \frac{z_n}{\mathcal{T}_n} \leq T_n, n \in \mathcal{N}, \tag{15a}$$

$$e_n z_n + \frac{z_n}{\mathcal{T}_n} \bar{P}_n \leq E_n, n \in \mathcal{N}, \tag{15b}$$

$$P_{n,k} \geq 0, n \in \mathcal{N}, k \in \mathcal{K}, \tag{15c}$$

$$\bar{P}_n \leq \bar{P}_{n,\text{tot}}, n \in \mathcal{N}, \tag{15d}$$

$$p_{\text{out},n,K} \leq \varepsilon_n, n \in \mathcal{N}, \tag{15e}$$

$$z_n (1 - l_n) = 0, z_n \geq 0, n \in \mathcal{N}, \tag{15f}$$

$$\sum_{n=1}^{N} l_n \leq B, n \in \mathcal{N}, \tag{15g}$$

$$l_n \in \{0, 1\}, n \in \mathcal{N}, \tag{15h}$$

where (15a) denotes that the total time consumption of user n should be no larger than the pre-determined time threshold T_n. Similarly, (15b) is used to ensure that the energy consumption can not exceed the available energy threshold E_n for user n. In addition, (15c) represents that the transmission power should be non-negative. Moreover, (15d) denotes that the total transmission power for each message delivery of user n is usually limited, and the total average transmission power should be no more than the maximum allowable average total transmission power threshold $\bar{P}_{n,\text{tot}}$. (15e) is the outage constraint. (15f) indicates that the sensed data is valid only when the user is selected for sensing the task. (15g) indicates that the maximum number of selected users is limited due to restricted resources. At last, (15h) is used to determine whether user n is selected.

In order to solve (15), the closed-form expression of the outage probability $p_{\text{out},n,K}$ needs to be obtained. However, the complex form of the exact outage expression still precludes the optimization of the problem (15). To address this issue, the simple form of asymptotic outage probabilities of the Type-I HARQ [44], HARQ-CC [45] and HARQ-IR [46] after K rounds in high signal-to-noise ratio (SNR) regime are obtained to ease the optimization of (15). Consequently, they can be unified as,

$$p_{\text{out},n,K} \simeq g_{n,K} \prod_{k=1}^{K} \frac{\sigma_{n,k}^2}{P_{n,k} \alpha_{n,k}^2}, \tag{16}$$

where $g_{n,K}$ is termed as the modulation and coding gain and expressed as

$$g_{n,K} = \begin{cases} \left(2^{R_n} - 1\right)^K, & \text{Type-I} \\ \frac{\left(2^{R_n} - 1\right)^K}{\Gamma(K+1)}, & \text{CC} \\ (-1)^K + 2^{R_n} \sum_{k=0}^{K-1} (-1)^k \frac{(R_n \ln 2)^{K-k-1}}{(K-k-1)!}, & \text{IR} \end{cases} \tag{17}$$

in which $\Gamma(\cdot)$ represents the Gamma function.

Despite utilizing the simplified form of asymptotic outage probabilities (16) to reduce computational complexity in the optimization process, it is important to note that the maximization problem (15) remains a non-convex optimization problem. This problem lacks explicit modality and a tractable form, making it difficult to solve. In this paper, we plan to address it in an efficient manner. The main ideas are expressed as follows: It was known that all users would have the opportunity to be selected for data sensing and transmission. Accordingly, the original optimization problem can be decomposed into N subproblems, each of which corresponds to the maximization of the reward for a single user. Since a_n is a constant in (14), the maximization of the reward is equivalent to the maximization of sensing data size. However, the maximization of sensing data size per user is also a challenging problem to solve. The difficulty mainly stems from the coupling between transmission power allocation and transmission rate selection. To tackle this problem, a divide-then-conquer method will be used. More precisely, we decompose the sensing data size maximization problem into two subproblems equivalently with regard to transmission power and transmission rate, respectively. After that, we obtain the optimal transmission rate and power by using the alternative optimization algorithm and Dinkelbach's algorithm. It is worth noting that not all users can be scheduled due to limited resources. After revisiting the original optimization problem, it can be observed that selecting the top-B users based on their achievable rewards results in the maximum system reward. Thus far, the original maximization problem is addressed. The detailed algorithm design will be sorted out in the following section.

IV. Algorithm Design

To elaborate on the detailed algorithm design for problem (15), we first simplify it by removing the user selection variable $\boldsymbol{l}$, considering that all users would have the opportunity to participate in the sensing task. Upon this assumption, the original problem (15) can be transformed into the following optimization problem:

$$\begin{aligned} \max_{\boldsymbol{z},\boldsymbol{R},\boldsymbol{P}} \quad & \mathcal{R} \\ \text{s.t.} \quad & \text{(15a)} - \text{(15e)}. \end{aligned} \tag{18}$$

The newly formulated optimization problem (18) can be further decomposed into N subproblems, each of which corresponds to the maximization of the reward $a_n \log(1 + z_n)$ for user n. Due to the fact that a_n is constant, maximizing the reward for an individual user is the same as maximizing the sensing data size z_n for that user. Therefore, problem (18) can be divided into N sensing data size maximization problem for a single user. Without loss of generality, we take user n as an example and formulate the maximization problem as follows:

$$\begin{aligned} \max_{R_n,\boldsymbol{P}_n} \quad & z_n \\ \text{s.t.} \quad & \text{(15a)} - \text{(15e)}. \end{aligned} \tag{19}$$

However, it is still difficult to solve (19) directly. The main difficulty is originated from the coupling between the transmission rate R_n and transmission power $\boldsymbol{P}_n$ in the constraints (15a) and (15b). To address this difficulty, we replace the average transmission power $\bar{P}_n$ in (15b) with the boundary value $\bar{P}_{n,\text{tot}}$ of (15d). As a result, (19) can be simplified as

follows:

$$\max_{R_n, \boldsymbol{P}_n} \quad z_n \tag{20}$$
$$\text{s.t.} \quad e_n z_n + \frac{z_n}{\mathcal{T}_n} \bar{P}_{n,\text{tot}} \leq E_n, n \in N, \tag{20a}$$
$$(15a), (15c) - (15e).$$

It is not difficult to verify that problem (20) achieves the optimal solution when the average transmission power $\bar{P}_n$ is maximized, specifically at the boundary value $\bar{P}_{n,\text{tot}}$. This equivalence can be substantiated in the numerical results section, demonstrating that (20) is equivalent to (19). Additionally, it can be observed that the sensing data size z_n depends on constraints (15a) and (20a). Taking into account these two constraints, we can derive the following relationships: $z_n \leq T_n / (1/o_n + 1/\mathcal{T}_n)$ and $z_n \leq E_n / \left(e_n + \bar{P}_{n,\text{tot}}/\mathcal{T}_n\right)$. By observing the two inequalities above, we can deduce that the optimal sensing data size z_n^* is achievable by maximizing LTAT, i.e., $\mathcal{T}_n$. Therefore, we can rewrite (20) as the following optimization problem:

$$\begin{aligned} \max_{R_n, \boldsymbol{P}_n} \quad & \mathcal{T}_n \\ \text{s.t.} \quad & (15c) - (15e). \end{aligned} \tag{21}$$

Note that (21) remains a non-convex optimization problem, which is challenging to solve directly due to the coupling among the optimization variables. To address this issue, we propose to use the divide-then-conquer manner. Specifically, we decompose problem (21) into two subproblems, namely, the transmission power allocation subproblem and the transmission rate selection subproblem. Then we dedicate to solving each of the two subproblems optimally in an efficient manner, and finally optimize the two types of optimization variables alternatively.

1) Transmission power allocation subproblem: In this section, given the transmission rate, i.e., R_n, the original optimization problem (21) degenerates to the transmission power allocation subproblem, whose mathematical formulation is given below:

$$\begin{aligned} \max_{\boldsymbol{P}_n} \quad & \mathcal{T}_n \\ \text{s.t.} \quad & (15c) - (15e). \end{aligned} \tag{22}$$

It can be observed that problem (22) is a fractional programming problem. To solve it, we propose to use the Dinkelbach's algorithm [47]. The Dinkelbach's algorithm is an iterative algorithm that transforms a concave-convex fractional programming problem into a sequence of convex optimization problems. By iteratively solving these convex subproblems, we can achieve convergence to the globally optimal solution of the original concave-convex fractional programming problem. It is worth nothing that Dinkelbach's algorithm has proven to be effective in obtaining the global optimal solution for problems expressed in concave-convex fractional form. Specifically, this form consists of a concave numerator and a convex denominator. However, (22) does not represent a concave-convex fractional form. This is because the numerator of $\mathcal{T}_n$, referred to as $A_n = R_n \left(1 - p_{\text{out},n,K}\right)$, is a non-concave function with respect to (w.r.t.) $\boldsymbol{P}_n$, while the denominator of $\mathcal{T}_n$, denoted by $B_n = \sum_{k=1}^{K} p_{\text{out},n,k-1}$, is a non-convex function w.r.t. $\boldsymbol{P}_n$. Fortunately, the following theorem can be utilized to resolve this issue.

Theorem 1. *Given* $P_{n,1}, \cdots, P_{n,j-1}, P_{n,j+1}, \cdots, P_{n,K}$, $p_{out,n,K}$ *is a decreasing and convex function w.r.t.* $P_{n,j}$ *for* $j \in \mathcal{K}$. *Accordingly,* A_n *and* B_n *are proved to be concave and convex functions of the* j*-th transmission power* $P_{n,j}$, *respectively. Therefore,* $\mathcal{T}_n$ *is a concave-convex fractional function w.r.t. the single-variable* $P_{n,j}$.

Proof: To prove the convexity of $p_{\text{out},n,K}$ w.r.t. $P_{n,j}$, it suffices to show that the second partial derivative of $p_{\text{out},n,K}$ w.r.t. $P_{n,j}$ is greater than or equal to zero. According to (16), it is evident that $p_{\text{out},n,K}$ is a decreasing function w.r.t. $P_{n,j}$ when $P_{n,1}, \cdots, P_{n,j-1}, P_{n,j+1}, \cdots, P_{n,K}$ are given. The first partial derivative of $p_{\text{out},n,K}$ w.r.t. $P_{n,j}$ satisfies $\frac{\partial p_{\text{out},n,K}}{\partial P_{n,j}} < 0$ and

$$\frac{\partial p_{\text{out},n,K}}{\partial P_{n,j}} = -g_{n,K} \frac{1}{P_{n,j}} \prod_{k=1}^{K} \frac{\sigma_{n,k}^2}{P_{n,k} \alpha_{n,k}^2}. \tag{23}$$

Then the second order partial derivative of $p_{\text{out},n,K}$ w.r.t. $P_{n,j}$ is calculated as

$$\frac{\partial^2 p_{\text{out},n,K}}{\partial P_{n,j}^2} = g_{n,K} \frac{2}{{P_{n,j}}^2} \prod_{k=1}^{K} \frac{\sigma_{n,k}^2}{P_{n,k} \alpha_{n,k}^2}. \tag{24}$$

It is clear that (24) is non-negative, so the convexity of $p_{\text{out},n,K}$ w.r.t. $P_{n,j}$ is proved successfully. Accordingly, A_n and B_n are concave and convex functions w.r.t. $P_{n,j}$, respectively. The proof is completed. ■

The findings in Theorem 1 enable us to solve (22) by virtue of alternately iterating optimization. Specifically, we decompose the original multi-variable optimization problem into a series of single-variable optimization problems. Then we dedicate to solving each of the single-variable optimization problems in an efficient manner, and finally optimize all transmission power variables alternately. To this end, without loss of generality, we consider the j-th transmission power $P_{n,j}$ as an example for analysis. As a result, given $P_{n,1}, \cdots, P_{n,j-1}, P_{n,j+1}, \cdots, P_{n,K}$, the individual optimization problem for the j-th transmission power $P_{n,j}$ is formulated as

$$\max_{P_{n,j}} \quad \mathcal{T}_n \tag{25}$$
$$\text{s.t.} \quad P_{n,j} > 0, \tag{25a}$$
$$(15d) \text{ and } (15e).$$

It can be observed that (25) is a fractional programming problem. In order to solve (25), Dinkelbach's algorithm is utilized to reformulate it as follows:

$$\max_{P_{n,j}} \quad A_n - \eta_{n,j} B_n \tag{26}$$
$$\text{s.t.} \quad P_{n,j} > 0, \tag{26a}$$
$$(15d) \text{ and } (15e),$$

with a new auxiliary variable $\eta_{n,j}$, which is iteratively updated as

$$\eta_{n,j}^{i+1} = \frac{A_n \left(P_{n,j}^i\right)}{B_n \left(P_{n,j}^i\right)}, \tag{27}$$

where i denotes the iteration index, and $P_{n,j}^{i}$ represents the i-th iterate transmission power that starts from an initial power $P_{n,j}^{0}$. It can be proven that convergence is guaranteed by alternately updating $\eta_{n,j}$ according to (27) and solving for $P_{n,j}^{i+1}$ in (26), because $\eta_{n,j}$ is non-decreasing after each iteration. Furthermore, it is worth nothing that the single-variable optimization problem (26) is a convex problem for fixed $\eta_{n,j}$. Thus, we can obtain the optimal solution $P_{n,j}^{*}$ for single-variable optimization problem (26). Algorithm 1 summarizes the details regarding single-variable optimization problem solution.

Algorithm 1: Optimal Single Transmision Power

input : The initial transmission power $P_{n,j}^{0}$. Assume the maximum iteration number to be $I_{\max}$.
output: $P_{n,j}^{*}$.

$i \leftarrow 0$.
repeat
Update $\eta_{n,j}^{i+1}$ in (27).
Calculate $P_{n,j}^{i+1}$ by solving problem (26).
$i \leftarrow i+1$.
until convergence or $i > I_{\max}$.
$P_{n,j}^{*} \leftarrow P_{n,j}^{i}$.

Lemma 1. *The time complexity of Algorithm 1 is $\mathcal{O}(I_{max})$. The convergence of Algorithm 1 is guaranteed.*

Proof: In Algorithm 1, during each round, $P_{n,j}^{i+1}$ is obtained by (26). To convergence, the worst case is that the maximum number of iterations is required. Accordingly, the time complexity can be obtained as $\mathcal{O}(I_{\max})$. Moreover, the convergence of Algorithm 1 is evident since the optimization problem (26) is convex. In addition, since the Algorithm 1 has at most $I_{\max}$ iterations in total, its convergence is ensured. The proof is completed. ∎

Thereafter, the alternating optimization method is devised to jointly optimize all transmission powers. We define $\left(\tilde{P}_{n,1}^{r},\cdots,\tilde{P}_{n,K}^{r}\right)$ as the iterate sequence in the r-th iteration that starts from initial powers $\left(\tilde{P}_{n,1}^{0},\cdots,\tilde{P}_{n,K}^{0}\right)$. When convergence conditions are met, the optimal solution $\left(\tilde{P}_{n,1}^{*},\cdots,\tilde{P}_{n,K}^{*}\right)$ of original problem (22) can be obtained. Details regarding our proposed solution are summarized in Algorithm 2.

Lemma 2. *The time complexity of Algorithm 2 is $\mathcal{O}(KR_{max}I_{max})$. The convergence of Algorithm 2 is ensured.*

Proof: Algorithm 2 involves K variables, i.e., $\tilde{P}_{n,1},\cdots,\tilde{P}_{n,K}$. Each variable $\tilde{P}_{n,k}, k\in[1,K]$ is updated by using Algorithm 1. To ensure convergence, the worst-case scenario is that updating a single variable and updating all variables may each require the maximum number of iterations. Therefore, the overall time complexity of Algorithm 2 can be calculated as $\mathcal{O}(KR_{\max}I_{\max})$, where the iteration number $R_{\max}$ is sufficiently large. In addition, the convergence of Algorithm 2 is guaranteed. Each variable is optimally solved by our designed Algorithm 1, which has been proven to be convergent. Moreover, the realizable LTAT is non-decreasing and has an upper bound. Therefore, Algorithm 2 is definitely convergent. The proof is completed. ∎

Algorithm 2: Transmission Power Allocation

input : The initial transmission powers $\left(\tilde{P}_{n,1}^{0},\cdots,\tilde{P}_{n,K}^{0}\right)$ and the maximum number of HARQ rounds K. Assume the maximum iteration number to be $R_{\max}$.
output: $\left(\tilde{P}_{n,1}^{*},\cdots,\tilde{P}_{n,K}^{*}\right)$.

$r \leftarrow 0$.
repeat
for $j=1$ **to** K **do**
By using Algorithm 1, find optimal transmission power $\tilde{P}_{n,j}^{r+1}$ under given $\tilde{P}_{n,1}^{r+1},\cdots,\tilde{P}_{n,j-1}^{r+1},\tilde{P}_{n,j+1}^{r},\cdots,\tilde{P}_{n,K}^{r}$.
end
$r \leftarrow r+1$.
until convergence or $r > R_{\max}$.
$\left(\tilde{P}_{n,1}^{*},\cdots,\tilde{P}_{n,K}^{*}\right) \leftarrow \left(\tilde{P}_{n,1}^{r},\cdots,\tilde{P}_{n,K}^{r}\right)$.

2) Transmission rate selection subproblem: Given the transmission power $\boldsymbol{P}_n$, the resultant problem is only related to the transmission rate R_n, which is expressed as follows:

$$\begin{aligned} \max_{R_n} \quad & \mathcal{T}_n, \\ \text{s.t.} \quad & \text{(15d) and (15e)}. \end{aligned} \tag{28}$$

Similar to (22), the optimization problem (28) is a concave-convex fractional problem in regard to R_n. Details are stated in the following lemma.

Theorem 2. *$p_{out,n,K}$ is an increasing and convex function w.r.t. R_n. Therefore, A_n and B_n can be proved to be concave and convex function w.r.t. R_n, respectively. Thus,* (28) *is a concave-convex fractional problem w.r.t. R_n.*

Proof: Please refer to Appendix A. ∎

Based on Theorem 2, (28) can be solved by using Dinkelbach's algorithm as well. To this end, we convert (28) into a convex optimization problem, and it is quoted below:

$$\begin{aligned} \max_{R_n} \quad & A_n - \beta_n B_n, \\ \text{s.t.} \quad & \text{(15d) and (15e)}, \end{aligned} \tag{29}$$

in which β_n is a new auxiliary variable that is iteratively updated as

$$\beta_n^{i+1} = \frac{A_n\left(R_n^{i}\right)}{B_n\left(R_n^{i}\right)}, \tag{30}$$

where R_n^{i} denotes the i-th iterate transmission rate that starts from an initial transmission rate R_n^{0}. Similar to (26), the convergence is guaranteed by alternatively updating β_n according to (30) and solving for R_n^{i+1} in (29). Thereupon, by solving the convex problem (29), the optimal transmission rate R_n^{*} of (28) can be obtained. Details regarding our proposed solution are summarised in Algorithm 3.

Lemma 3. *The time complexity of Algorithm 3 is $\mathcal{O}(I_{max})$. The convergence of Algorithm 3 is ensured.*

Proof: Algorithm 3 is similar to Algorithm 1, and the optimization problem (29) in Algorithm 3 is convex, thus the

Algorithm 3: Optimal Transmission Rate Allocation

input : The initial transmission rate R_n^0. Assume the maximum iteration number to be $I_{\max}$.
output: R_n^*.

$i \leftarrow 0$.
repeat
Update β_n^{i+1} in (30).
Calculate R_n^{i+1} by solving problem (29).
$i \leftarrow i+1$.
until convergence or $i > I_{\max}$.
$R_n^* \leftarrow R_n^i$.

time complexity of Algorithm 3 is $\mathcal{O}(I_{\max})$. Based on above analysis, the convergence of Algorithm 3 also can be ensured. The proof is completed. ■

3) Alternating optimization algorithm for the joint transmission power-rate problem: Thus far, we have explained how the two subproblems can be optimally solved. In this section, an alternating optimization approach is devised to jointly optimize the transmission power $\boldsymbol{P}_n$ and rate R_n. We denote $\hat{\boldsymbol{P}}_n^m$ and $\hat{R}_n^m$ as the transmission power allocation strategy as well as the transmission rate design strategy in the m-th iteration. By substituting $\hat{\boldsymbol{P}}_n^m$ and $\hat{R}_n^m$ into (11), we obtain $\mathcal{T}_n^m$. Moreover, we assume that $\hat{\boldsymbol{P}}_n^0$ and $\hat{R}_n^0$ are set by using the top-preference scheme. When convergence conditions are met, the optimal solution $\hat{\boldsymbol{P}}_n^*$ and $\hat{R}_n^*$ of original problem (21) can be obtained. Consequently, $\mathcal{T}_n^*$ is also obtained by (11). With these definitions, the description of our joint optimization method is summarized in Algorithm 4.

Algorithm 4: Joint Optimization Algorithm

input : The initial transmission power set $\hat{\boldsymbol{P}}_n^0$ and transmission rate $\hat{R}_n^0$. Assume the maximum iteration number to be $M_{\max}$.
output: $\hat{\boldsymbol{P}}_n^*$, $\hat{R}_n^*$, $\mathcal{T}_n^*$.

$m \leftarrow 0$.
repeat
For $n \in \mathcal{N}$, find its optimal transmission powers strategy, i.e., $\hat{\boldsymbol{P}}_n^{m+1}$, based on Algorithm 2 under given $\hat{R}_n^m$.
Update the transmission rate strategy as $\hat{R}_n^{m+1}$ by using Algorithm 3 for fixed $\hat{\boldsymbol{P}}_n^m$.
Substitute $\hat{\boldsymbol{P}}_n^{m+1}$ and $\hat{R}_n^{m+1}$ into (11) for obtaining $\mathcal{T}_n^{m+1}$.
$m \leftarrow m+1$.
until convergence or $m > M_{\max}$.
$\hat{\boldsymbol{P}}_n^* \leftarrow \hat{\boldsymbol{P}}_n^m$, $\hat{R}_n^* \leftarrow \hat{R}_n^m$, $\mathcal{T}_n^* \leftarrow \mathcal{T}_n^m$.

Lemma 4. *The time complexity of Algorithm 4 is $\mathcal{O}(KR_{max}I_{max}M_{max})$. The convergence of Algorithm 4 is guaranteed.*

Proof: The time complexity of Algorithm 4 depends on the computational complexity regarding Algorithm 2 and Algorithm 3. They are $\mathcal{O}(KR_{\max}I_{\max})$ and $\mathcal{O}(I_{\max})$, respectively. Thus, the time complexity of Algorithm 4 is $\mathcal{O}(\max\{KR_{\max}I_{\max}, I_{\max}\}M_{\max}) = \mathcal{O}(KR_{\max}I_{\max}M_{\max})$. Furthermore, the convergence of Algorithm 4 is ensured [48]. Its convergence properties can be proved by a similar methodology to Algorithm 2. The proof is completed. ■

Although the convergence regarding the developed solutions for the original maximization problem is proved, we cannot ensure the global optimality of the Algorithm 4 as the considered optimization problem is non-convex, and lacks of modular properties. However, the proposed solutions have tolerate time complexity, which has great implications for the real communication systems.

Based on Algorithm 4, we can get the optimal LTAT $\mathcal{T}_n^*$ for single user n. Thereafter, by utilizing the inequalities $z_n \leq T_n/\left(1/o_n + 1/\mathcal{T}_n\right)$ and $z_n \leq E_n/\left(e_n + \bar{P}_{n,\text{tot}}/\mathcal{T}_n\right)$, the optimal data size z_n^* of user n can be obtained. However, as shown in (1), not all users can participate in data sensing and transmission due to limited resources. We only need to choose the users whose achievable reward, represented by $a_n \cdot \log(1+z_n)$, ranks in top B. In this way, the user selection vector $\boldsymbol{l}$ can be determined.

V. Numerical Results

In this section, extensive numerical simulations are performed to demonstrate the effectiveness of our proposed HARQ-aided MCS scheme. We consider a HARQ-aided MCS system comprising one BS and an edge server serving 20 users, i.e., $N = 20$. To facilitate clarity, the system parameters used throughout the paper are summarized in Table II.

TABLE II: System parameter settings.

Notation	Description	Value
N	Mobile users	20
B	The number of subchannels	$5-10$
K	The maximum HARQ rounds	3
$\sigma_{n,k}^2$	Noise variance	1
$\alpha_{n,k}^2$	Channel power gain	$2-4$
o_n	Sensing data rate of user n	$10^6 - 10^5$ bits/s [21]
e_n	Sensing energy consumption per bit	10^{-12} J/bit
T_n	Time threshold of user n	$1-10$ s [21]
E_n	Energy threshold of user n	$0.2-2$ J [21]
$\bar{P}_{n,\text{tot}}$	Maximum transmit power	$0.1-0.2$ W
c_n	Reward coefficient	1.5
ϵ_n	Outage probability threshold	$10^{-8}-1$

We utilize the labels "Type-I", "CC", and "IR" to represent the Type-I HARQ, HARQ-CC, and HARQ-IR schemes, respectively, which assist the MCS system in achieving reliable transmission. Furthermore, the following benchmark strategies are taken into account for performance comparison:

- UC: In this approach, Type-I HARQ is utilized to enhance the reliability of MCS system. To ensure a fair comparison, the data sensing size of each user is optimized using our proposed Algorithm 4. However, the selection of users is based on choosing those with better channel conditions.
- SC: Similarly to the UC approach, Type-I HARQ is used in this baseline to improve the reliability of the MCS system. However, in this strategy, the selection of users is based on choosing those with better sensing abilities.
- PR: In this approach, the selection of transmission power and rate follows a descending order from large to small under constrained conditions. As a result, we can determine the corresponding sensing data size and reward.

In Fig. 2, the optimal reward of agent is plotted against the outage probability tolerance ϵ. We set $B = 10$, $\bar{P}_{n,\text{tot}} = 0.2$ W, $T_n = 5$ s and $E_n = 1.5$ J. It is observed that the optimal reward of HARQ-IR-aided MCS system is better than that of other baselines. This observation demonstrates the effectiveness of our algorithm and the superiority of the HARQ-IR technique. In addition, the optimal rewards for IR and CC exhibit a high degree of similarity at low-to-medium outage probability. This is due to the fact that the experimental results are obtained under low SNR conditions, and both CC and IR show considerable transmission reliability under low SNR conditions. The reward difference between IR and CC amplifies as SNR increases. Moreover, the optimal reward of all baselines converges to a performance bound under loose outage constraint, i.e., $\epsilon \to 1$. Furthermore, it is revealed that the optimal reward of Type-I and UC are in perfect agreement. This is due to the fact that the users with superior channel conditions are more likely to be selected. The key difference between UC and Type-I HARQ lies in user selection methods. In UC, user selection is based on identifying users with the best channel conditions. In contrast, Type-I HARQ focuses on identifying users with the highest achievable reward. Therefore, choosing the user with the largest available reward is effectively the same as selecting the user with the best channel conditions.

The observations indicate that the users with superior channel conditions are more likely to be selected.

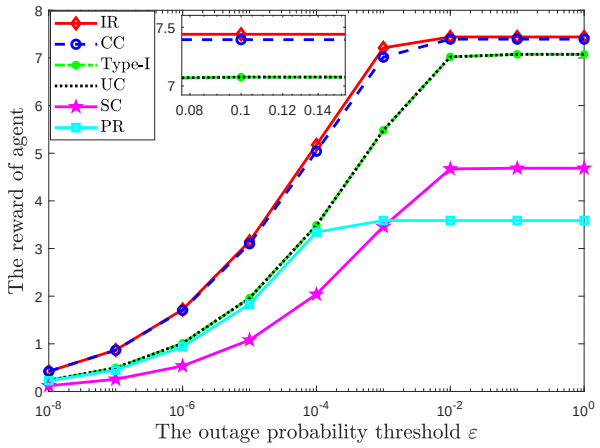

Fig. 2: Agent's reward versus the outage probability threshold ϵ.

Fig. 3 investigates the optimal reward of agent against the maximum transmit power $\bar{P}_{n,\text{tot}}, n \in \mathcal{N}$. All users have the same maximum transmit power. We set $B = 10$, $\epsilon = 10^{-6}$, $T_n = 5$ s, and $E_n = 1.5$ J. According to Fig. 3, we observe that the optimal rewards of all schemes are proportional to the transmission power threshold $\bar{P}_{n,\text{tot}}$, which also validates the correctness of our previous operation of taking the average transmission power $\bar{P}_n$ as a boundary value $\bar{P}_{n,\text{tot}}$. Moreover, the rewards of IR and CC are significantly higher than those of other strategies, which demonstrate the effectiveness of our proposed algorithm and the superiority of HARQ-IR and HARQ-CC technologies. In addition, the similar results between Type-I and UC can be attributed to the selection of users with better channel conditions. Besides, the results of UC and SC indicate a trade-off between the channel conditions and sensing abilities. Moreover, the similarity in results between SC and PR is due to the fact that in our parameter settings, users with the best channel conditions have the worst sensing abilities.

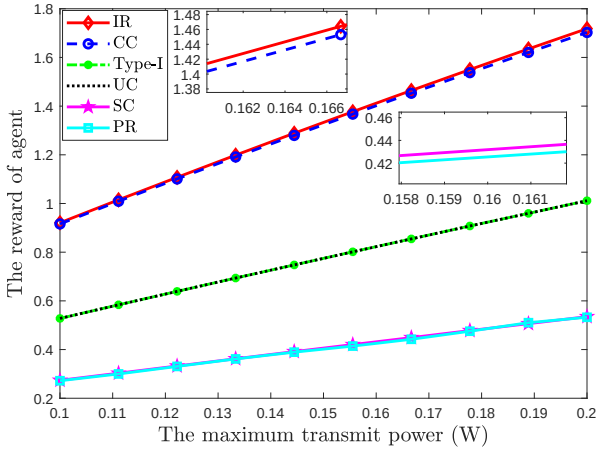

Fig. 3: Agent's reward versus the maximum transmit power.

The relationship of reward and time threshold T_n is plotted in Fig. 4, where the time thresholds of all users are the same. Therein, we set $B = 10$, $\epsilon = 10^{-6}$, $\bar{P}_{n,\text{tot}} = 0.2$, and $E_n = 1.5$. The "MR" policy is modified from the optimal transmit power and sensing data size algorithm presented in [22]. Specifically, "MR" determines the transmission power allocation and sensing data size optimization according to [22], and the bandwidth is a normalized one. It is obvious that the optimal reward of "MR" outperforms our strategy. This advantage stems from the assumption of perfect transmission, as the "MR" method does not account for transmission failures, which significantly reduces latency. The differences in results arise not from the algorithm itself but from the varying settings of the system model. In addition, it is readily found that the optimal rewards of IR and CC under different time thresholds T_n outperform dramatically the other strategies, demonstrating the effectiveness of our proposed algorithm and the superiority of HARQ-IR and HARQ-CC. In addition, the outcomes of all strategies converge to the performance bound under a loose time constraint. This is due to the fact that, with the relaxation of time constraints, the system's performance is ultimately constrained by the allocation of energy resources. We also find that the results of other benchmarks are better than those of PR, which indicates the effectiveness of our proposed algorithm for optimizing transmission power and rate. Moreover, it is evident that the results for Type-I and UC are similar. This similarity is due to the same reasons outlined in Fig. 2.

Fig. 5 shows how the agent's reward changes with the available number of subchannels. We set $\epsilon = 10^{-6}$, $\bar{P}_{n,\text{tot}} = 0.2$ W, $T_n = 5$ s, and $E_n = 1.5$ J. We can observe that the agent's reward increases with the number of subchannels. This is because more available channels in the network can always

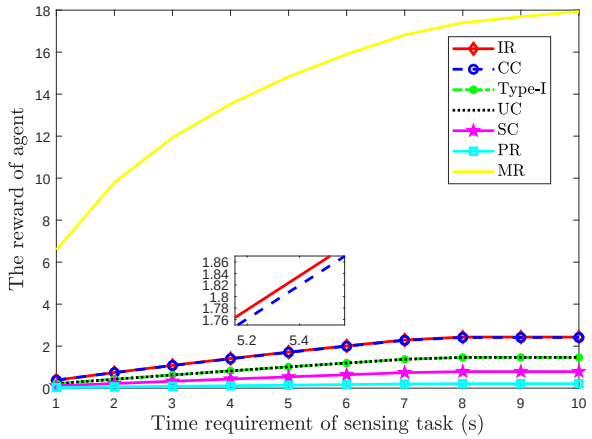

Fig. 4: Agent's reward versus sensing task's time requirement.

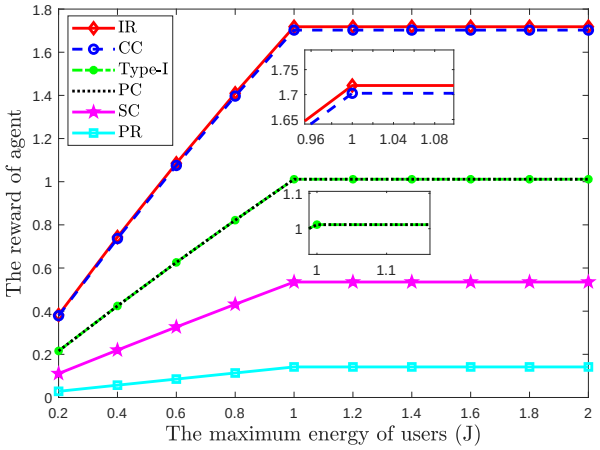

Fig. 6: Agent's reward versus the maximum energy.

lead to more users being selected for the sensing task. Besides, the improvement of PR strategy is relatively small because the allocation of transmission powers and transmission rates under PR policy is limited to small values. In addition, the results for UC and Type-I HARQ are consistent for the same reasons presented in Fig. 2.

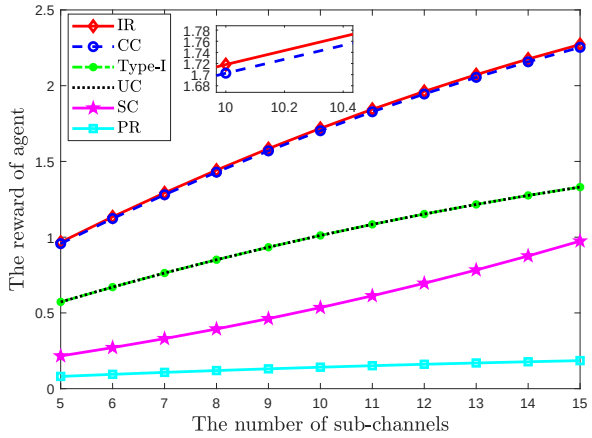

Fig. 5: Agent's reward versus available wireless bandwidth.

In Fig. 6, the agents reward is examined versus the maximum energy of users (denoted as E_n) with $\epsilon = 10^{-6}$, $\bar{P}_{n,\text{tot}} = 0.2$ Watt, $T_n = 5$ s, and $B = 10$. We can see that HARQ-IR technique and our proposed policy provide the best performance. Additionally, a noticeable observation is that the agent's reward demonstrates a positive correlation with the maximum energy of users when the maximum energy remains below 1. Conversely, when the maximum energy exceeds 1, the agent's reward converges towards a performance bound. This phenomenon can be attributed to the fact that the system's performance is constrained by the allocation of time resources. Moreover, the consistent results for UC and Type-I HARQ can be attributed to the reasons presented in Fig. 2.

The optimal sensing time of a specific user (i.e., user 1) changes with its available energy is investigated in Fig. 7. We set the sensing task time requirement T_n to 10 seconds, vary the energy of user 1, and keep the parameters of other users fixed. In Fig. 7, it is notable that only four baselines are present. This is due to the fact that the algorithms used in PC and SC are identical to Type-I, except for the difference in user selection methods. However, since this experiment does not illustrate user selection, PC and SC are not included as baselines. From Fig. 7, we can see that the optimal sensing duration increases with the energy of the user. This is because larger energy usually leads to a larger transmission power and sensing data size. Futhermore, it is evident that the optimal sensing time of user 1 under the IR strategy is larger than that of other baselines. This observation indicates that the optimal sensing data size of user 1 under IR strategy is better than that of other baselines.

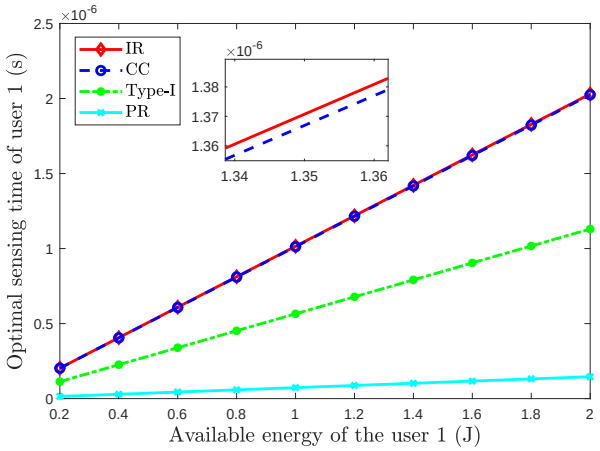

Fig. 7: Optimal sensing time versus the available energy.

VI. Conclusion

In this paper, we proposed a framework for a resource-constrained HARQ-aided MCS system to ensure reliable data transmission. The framework was designed to integrate joint sensing and communication, taking advantage of HARQ to enhance the reliability of data transmission. Our primary

objective was to maximize the system's reward while satisfying the constraints imposed by limited resources and latency requirement. The considered problem was a non-convex, mixed-integer programming problem. To facilitate the analysis, we initially considered that all users would have the opportunity to participate in the sensing task. Based on this consideration, the original problem was transferred into the LTAT maximization problem. Recognizing the coupling between transmission power and rate, we devised an efficient divide-then-conquer approach. This approach allowed us to decompose the problem into two subproblems. To solve each non-convex fractional programming subproblem, Dinkelbatch's algorithm and alternating iteration algorithm were employed. At last, we ranked the users in descending order based on their optimal achievable reward and selected the top-B users to complete the user selection process. Extensive numerical results verified the superiority of our developed algorithm compared to various baseline schemes. In future, we plan to study the joint transmission, communication and computation problems for HARQ-aided MCS systems.

Appendix A
Proof of Theorem 2

To complete the proof, it suffices to verify that the first and the second partial derivatives of $p_{\text{out},n,K}$ w.r.t. R_n are greater than or equal to zero. To begin with, it is readily found that $p_{\text{out},n,K}$ is an increasing function of R_n. This is due to the fact that as R_n increases, the outage probability (6) also increases. Therefore, according to (16), the first partial derivative of $p_{\text{out},n,K}$ satisfies $\frac{\partial p_{\text{out},n,K}}{\partial R_n} \geq 0$ and is

$$\frac{\partial p_{\text{out},n,K}}{\partial R_n} = \frac{\partial g_{n,K}}{\partial R_n} \prod_{k=1}^{K} \frac{\sigma_{n,k}^2}{P_{n,k}\alpha_{n,k}^2}, \tag{31}$$

where $\frac{\partial g_{n,K}}{\partial R_n}$ is

$$\frac{\partial g_{n,K}}{\partial R_n} = \begin{cases} \ln 2K\left(2^{R_n}-1\right)^{K-1}2^{R_n}, & \text{Type-I} \\ \frac{\ln 2K\left(2^{R_n}-1\right)^{K-1}2^{R_n}}{\Gamma(K+1)}, & \text{CC} \\ \frac{2^{R_n}\ln 2(R_n\ln 2)^{K-1}}{(K-1)!}. & \text{IR} \end{cases} \tag{32}$$

Since $\frac{\partial p_{\text{out},n,K}}{\partial R_n} \geq 0$, we have $\frac{\partial g_{n,K}}{\partial R_n} \geq 0$. Taking the second partial derivatives of $p_{\text{out},n,K}$ w.r.t. R_n yields

$$\frac{\partial^2 p_{\text{out},n,K}}{\partial R_n^2} = \frac{\partial^2 g_{n,K}}{\partial R_n^2} \prod_{k=1}^{K} \frac{\sigma_{n,k}^2}{P_{n,k}\alpha_{n,k}^2}, \tag{33}$$

and $\frac{\partial^2 g_{n,K}}{\partial R_n^2}$ is given below:

$$\frac{\partial^2 g_{n,K}}{\partial R_n^2} = \begin{cases} 2^{R_n}(\ln 2)^2K\left(2^{R_n}-1\right)^{K-2}\left(2^{R_n}K-1\right), & \text{Type-I} \\ \frac{2^{R_n}(\ln 2)^2K\left(2^{R_n}-1\right)^{K-2}\left(2^{R_n}K-1\right)}{\Gamma(K+1)}, & \text{CC} \\ \frac{(\ln 2)^2\left(2^{R_n}(R_n\ln 2)^{K-1}+(K-1)2^{R_n}(R_n\ln 2)^{K-2}\right)}{(K-1)!}. & \text{IR} \end{cases} \tag{34}$$

With the non-negativity of $\frac{\partial g_{n,K}}{\partial R_n}$ in (32), (34) indicates that $\frac{\partial^2 g_{n,K}}{\partial R_n^2} \geq 0$. Thus $\frac{\partial^2 p_{\text{out},n,K}}{\partial R_n^2} \geq 0$, and the convexity of $p_{\text{out},n,K}$ w.r.t. R_n is proved.

It is not difficult to observe that B_n is a convex function w.r.t. R_n. Subsequently, we prove the concavity of A_n. As for A_n, the first order partial derivative of A_n w.r.t. R_n is expressed as follows:

$$\frac{\partial A_n}{\partial R_n} = 1 - p_{\text{out},n,K} - R_n\frac{\partial p_{\text{out},n,K}}{\partial R_n}. \tag{35}$$

Taking the second order partial derivative of A_n w.r.t. R_n yields

$$\frac{\partial^2 A_n}{\partial R_n^2} = -R_n\frac{\partial^2 p_{\text{out},n,K}}{\partial R_n^2}. \tag{36}$$

With the non-negativity of $\frac{\partial^2 p_{\text{out},n,K}}{\partial R_n^2}$, (36) indicates that $\frac{\partial^2 A_n}{\partial R_n^2} \leq 0$. Thus the concavity of A_n is proved. Therefore, $\mathcal{T}_n = A_n/B_n$ is a concave-convex fractional function w.r.t. R_n. The proof is eventually completed.

References

[1] Y. Fu, Y. Shan, Q. Zhu, K. Hung, Y. Wu, and T. Q. S. Quek, "A distributed microservice-aware paradigm for 6G: Challenges, principles, and research opportunities," *IEEE Network*, vol. 38, no. 3, pp. 163–170, May 2024.

[2] P. Zhou, Y. Zheng, and M. Li, "How long to wait? predicting bus arrival time with mobile phone based participatory sensing," *IEEE Trans. Mobile Comput.*, vol. 13, no. 6, pp. 1228–1241, Aug. 2014.

[3] L. Shu, Y. Chen, Z. Huo, N. Bergmann, and L. Wang, "When mobile crowd sensing meets traditional industry," *IEEE Access*, vol. 5, pp. 15 300–15 307, Jan. 2017.

[4] R. K. Ganti, F. Ye, and H. Lei, "Mobile crowdsensing: current state and future challenges," *IEEE Commun. Mag.*, vol. 49, no. 11, pp. 32–39, Nov. 2011.

[5] Y. Fu, Y. Zhang, Q. Zhu, H. Dai, M. Li, and T. Q. S. Quek, "A new vision of wireless edge caching networks (WECNs): Issues, technologies, and open research trends," *IEEE Network*, vol. 38, no. 1, pp. 247–253, Jan. 2024.

[6] H. Ma, D. Zhao, and P. Yuan, "Opportunities in mobile crowd sensing," *IEEE Commun. Mag.*, vol. 52, no. 8, pp. 29–35, Aug. 2014.

[7] A. Capponi, C. Fiandrino, B. Kantarci, L. Foschini, D. Kliazovich, and P. Bouvry, "A survey on mobile crowdsensing systems: Challenges, solutions, and opportunities," *IEEE Commun. Surveys. Tuts*, vol. 21, no. 3, pp. 2419–2465, Apr. 2019.

[8] P. Zhou, W. Chen, S. Ji, H. Jiang, L. Yu, and D. Wu, "Privacy-preserving online task allocation in edge-computing-enabled massive crowdsensing," *IEEE Internet Things J.*, vol. 6, no. 5, pp. 7773–7787, Oct. 2019.

[9] M. Marjanovi, A. Antoni, and I. P. arko, "Edge computing architecture for mobile crowdsensing," *IEEE Access*, vol. 6, pp. 10 662–10 674, Jan. 2018.

[10] Z. Li, Z. Song, and X. Chen, "Privacy-preserving cost minimization in mobile crowd sensing supported by edge computing," *IEEE Access*, vol. 8, pp. 121 920–121 928, Jul. 2020.

[11] H. Li, T. Li, W. Wang, and Y. Wang, "Dynamic participant selection for large-scale mobile crowd sensing," *IEEE Trans. Mobile Comput.*, vol. 18, no. 12, pp. 2842–2855, Dec. 2019.

[12] C. Fiandrino, F. Anjomshoa, B. Kantarci, D. Kliazovich, P. Bouvry, and J. N. Matthews, "Sociability-driven framework for data acquisition in mobile crowdsensing over fog computing platforms for smart cities," *IEEE Trans. Sustain. Comput.*, vol. 2, no. 4, pp. 345–358, Oct. 2017.

[13] H. Jin, L. Su, D. Chen, H. Guo, K. Nahrstedt, and J. Xu, "Thanos: Incentive mechanism with quality awareness for mobile crowd sensing," *IEEE Trans. Mobile Comput.*, vol. 18, no. 8, pp. 1951–1964, Aug. 2019.

[14] C. Lai and X. Zhang, "Duration-sensitive task allocation for mobile crowd sensing," *IEEE Syst. J.*, vol. 14, no. 3, pp. 4430–4441, Feb. 2020.

[15] S. Yu, X. Chen, S. Wang, L. Pu, and D. Wu, "An edge computing-based photo crowdsourcing framework for real-time 3D reconstruction," *IEEE Trans. Mobile Comput.*, vol. 21, no. 2, pp. 421–432, Feb. 2022.

[16] S. Xu, X. Chen, X. Pi, C. Joe-Wong, P. Zhang, and H. Y. Noh, "iLOCuS: Incentivizing vehicle mobility to optimize sensing distribution in crowd sensing," *IEEE Trans. Mobile Comput.*, vol. 19, no. 8, pp. 1831–1847, Nov. 2020.

[17] H. Jin, B. He, L. Su, K. Nahrstedt, and X. Wang, "Data-driven pricing for sensing effort elicitation in mobile crowd sensing systems," *IEEE/ACM Trans. Netw.*, vol. 27, no. 6, pp. 2208–2221, Dec. 2019.

[18] Y. Liu, B. Guo, Y. Wang, W. Wu, Z. Yu, and D. Zhang, "Taskme: Multi-task allocation in mobile crowd sensing," in *Proc. ACM int. joint conf. pervasive ubiquitous comput.*, Feb. 2016, pp. 403–414.

[19] J. Wang, Y. Wang, D. Zhang, F. Wang, H. Xiong, C. Chen, Q. Lv, and Z. Qiu, "Multi-task allocation in mobile crowd sensing with individual task quality assurance," *IEEE Trans. Mobile Comput.*, vol. 17, no. 9, pp. 2101–2113, Nov. 2018.

[20] Z. Zhou, X. Li, C. You, K. Huang, and Y. Gong, "Joint sensing and communication-rate control for energy efficient mobile crowd sensing," *IEEE Trans. Wireless Commun.*, vol. 22, no. 2, pp. 1314–1327, Feb. 2023.

[21] X. Li, C. You, S. Andreev, Y. Gong, and K. Huang, "Wirelessly powered crowd sensing: Joint power transfer, sensing, compression, and transmission," *IEEE J. Sel. Areas Commun.*, vol. 37, no. 2, pp. 391–406, Feb. 2019.

[22] X. Li, G. Feng, Y. Sun, S. Qin, and Y. Liu, "A unified framework for joint sensing and communication in resource constrained mobile edge networks," *IEEE Trans. Mobile Comput.*, vol. 22, no. 10, pp. 5643–5656, Oct. 2023.

[23] T. Cai, Z. Yang, Y. Chen, W. Chen, Z. Zheng, Y. Yu, and H.-N. Dai, "Cooperative data sensing and computation offloading in UAV-assisted crowdsensing with multi-agent deep reinforcement learning," *IEEE Trans. Netw. Sci. Eng.*, vol. 9, no. 5, pp. 3197–3211, Apr. 2021.

[24] A. Ray, S. Mallick, S. Mondal, S. Paul, C. Chowdhury, and S. Roy, "A framework for mobile crowd sensing and computing based systems," in *Proc. IEEE Int. Conf. Advanced Net. Telecommun. Systems (ANTS)*. Indore, India, May 2018, pp. 1–6.

[25] X. Li, G. Feng, Y. Liu, S. Qin, and Z. Zhang, "Joint sensing, communication, and computation in mobile crowdsensing enabled edge networks," *IEEE Trans. Wireless Commun.*, vol. 22, no. 4, pp. 2818–2832, Apr. 2023.

[26] M. Le, D. T. Hoang, D. N. Nguyen, W.-J. Hwang, and Q.-V. Pham, "Wirelessly powered federated learning networks: Joint power transfer, data sensing, model training, and resource allocation," *IEEE Internet Things J.*, Oct. 2023.

[27] X. Xie, T. Bai, W. Guo, Z. Wang, and A. Nallanathan, "Cooperative computing for mobile crowdsensing: Design and optimization," *IEEE Trans. Mobile Comput.*, vol. 23, no. 5, pp. 6437–6454, Oct. 2023.

[28] H. Ren, K. Wang, and C. Pan, "Intelligent reflecting surface-aided URLLC in a factory automation scenario," *IEEE Trans. Commun.*, vol. 70, no. 1, pp. 707–723, Jan. 2022.

[29] Z. Zhou, J. Feng, B. Gu, B. Ai, S. Mumtaz, J. Rodriguez, and M. Guizani, "When mobile crowd sensing meets UAV: Energy-efficient task assignment and route planning," *IEEE Trans. Commun.*, vol. 66, no. 11, pp. 5526–5538, Nov. 2018.

[30] W. Saad, M. Bennis, and M. Chen, "A vision of 6G wireless systems: Applications, trends, technologies, and open research problems," *IEEE Netw.*, vol. 34, no. 3, pp. 134–142, Jun. 2020.

[31] A. Ahmed, A. Al-Dweik, Y. Iraqi, H. Mukhtar, M. Naeem, and E. Hossain, "Hybrid automatic repeat request (HARQ) in wireless communications systems and standards: A contemporary survey," *IEEE Commun. Surv. Tut.*, vol. 23, no. 4, pp. 2711–2752, Jul. 2021.

[32] L. Tan, Z. Kuang, L. Zhao, and A. Liu, "Energy-efficient joint task offloading and resource allocation in OFDMA-based collaborative edge computing," *IEEE Trans. Wireless Commun.*, vol. 21, no. 3, pp. 1960–1972, Sep. 2021.

[33] P.-Q. Huang, Y. Wang, K. Wang, and Z.-Z. Liu, "A bilevel optimization approach for joint offloading decision and resource allocation in cooperative mobile edge computing," *IEEE trans. cybern.*, vol. 50, no. 10, pp. 4228–4241, Jun. 2019.

[34] G. Caire and D. Tuninetti, "The throughput of hybrid-ARQ protocols for the gaussian collision channel," *IEEE Trans. Inf. Theory*, vol. 47, no. 5, pp. 1971–1988, Jul. 2001.

[35] H. Ding, S. Ma, C. Xing, Z. Fei, Y. Zhou, and C. P. Chen, "Analysis of hybrid ARQ in ad hoc networks with correlated interference and feedback errors," *IEEE trans. wireless commun.*, vol. 12, no. 8, pp. 3942–3955, Aug. 2013.

[36] R. Bhattacharya, L. Lin, and V. Patrangenaru, *A course in mathematical statistics and large sample theory*. New York, NY: Springer New York, 2016.

[37] A. Chelli, E. Zedini, M.-S. Alouini, J. R. Barry, and M. Ptzold, "Performance and delay analysis of hybrid ARQ with incremental redundancy over double Rayleigh fading channels," *IEEE Trans. Wireless Commun.*, vol. 13, no. 11, pp. 6245–6258, Nov. 2014.

[38] Z. Shi, S. Ma, G. Yang, and M.-S. Alouini, "Energy-efficient optimization for HARQ schemes over time-correlated fading channels," *IEEE Trans. Veh. Technol.*, vol. 67, no. 6, pp. 4939–4953, Mar. 2018.

[39] S. He, D.-H. Shin, J. Zhang, and J. Chen, "Toward optimal allocation of location dependent tasks in crowdsensing," in *Proc. IEEE Int. Conf. Comput. Commun. (INFOCOM)*. Toronto, Canada, Apr. 2014, pp. 745–753.

[40] D. Yang, G. Xue, X. Fang, and J. Tang, "Crowdsourcing to smartphones: Incentive mechanism design for mobile phone sensing," in *Proc. 18th Annu. Int. Conf. Mobile Comput. Netw.* Istanbul, Turkey, Aug. 2012, pp. 173–184.

[41] J. C. Russ, *The image processing handbook*. USA: CRC press, 2006.

[42] C. M. Bishop and N. M. Nasrabadi, *Pattern recognition and machine learning*. Springer, 2006, vol. 4, no. 4.

[43] X. Zhang, Z. Yang, W. Sun, Y. Liu, S. Tang, K. Xing, and X. Mao, "Incentives for mobile crowd sensing: A survey," *IEEE Commun Surveys Tuts.*, vol. 18, no. 1, pp. 54–67, Mar. 2016.

[44] H. Wang, Z. Shi, Y. Fu, and R. Song, "Outage performance for NOMA-aided small cell networks with HARQ," *IEEE Wirel. Commun.*, vol. 10, no. 1, pp. 72–76, Jan. 2021.

[45] Z. Shi, S. Ma, F. Hou, K.-W. Tam, and Y.-C. Wu, "Optimal power allocation for HARQ schemes over time-correlated Nakagami-m fading channels," in *Proc. IEEE/CIC Int. Conf. Commun. China,*. Shenzhen, China, Dec. 2016, pp. 1–6.

[46] Z. Shi, H. Wang, Y. Fu, X. Ye, G. Yang, and S. Ma, "Outage performance and AoI minimization of HARQ-IR-RIS aided IoT networks," *IEEE Trans. Commun.*, vol. 3, no. 71, pp. 1740–1754, Mar. 2023.

[47] K. Shen and W. Yu, "Fractional programming for communication systemsPart I: Power control and beamforming," *IEEE Trans. Signal Process.*, vol. 66, no. 10, pp. 2616–2630, Jun. 2018.

[48] R. G. Bartle and D. R. Sherbert, *Introduction to real analysis*. Wiley New York, 2000, vol. 2.

Jiahui Feng received her B.S. degree in internet of things engineering from Jinan University, China, in 2020 and her M.S. degree in electronic and communication engineering from Jinan University, China, in 2023. She is currently working toward the Ph.D. degree with the School of Science and Technology, Hong Kong Metropolitan University (HKMU). Her current research interests include hybrid automatic repeat request, mobile crowdsensing, and edge computing.

Yaru Fu (S'14-M'18) received her Ph.D in Electronic Engineering from City University of Hong Kong (CityU) in 2018. She is currently an Assistant Professor with School of Science and Technology, Hong Kong Metropolitan University (HKMU). She is presently serving as an Associate Editor for the IEEE TRANSACTIONS ON COGNITIVE COMMUNICATIONS AND NETWORKING, the IEEE INTERNET OF THINGS JOURNAL, the IEEE WIRELESS COMMUNICATIONS LETTERS, the IEEE NETWORKING LETTERS, and the SPRINGER NATURE COMPUTER SCIENCE. She also serves as a Review Editor for the FRONTIERS IN COMMUNICATIONS & NETWORKS, a Guest Editor for the SPACE: SCIENCE & TECHNOLOGY, and a Leading Guest Editor for the ELECTRONICS.

Dr. Fu was honored with the 2021 Katie Shu Sui Pui Charitable Trust - Outstanding Research Publication Award (Gold Prize), 2022 Best Editor Award for IEEE WIRELESS COMMUNICATIONS LETTERS, 2022 Katie Shu Sui Pui Charitable Trust - Excellent Research Publication Award, 2022 Exemplary Reviewer for the IEEE TRANSACTIONS ON COMMUNICATIONS (fewer than 5%), and 2023 Katie Shu Sui Pui Charitable Trust - President's Research Excellence Award. She was listed on the World's Top 2% Scientists 2023 ranking by Stanford University in the United States. Her research interests include intelligent wireless communications and networking, mobile edge computing, and digital twin.

Zheng Shi received his B.S. degree in communication engineering from Anhui Normal University, China, in 2010 and his M.S. degree in communication and information system from Nanjing University of Posts and Telecommunications (NUPT), China, in 2013. He obtained his Ph.D. degree in Electrical and Computer Engineering from University of Macau, Macao, in 2017. He is currently an Associate Professor with the School of Intelligent Systems Science and Engineering, Jinan University, Zhuhai, China. His current research interests include hybrid automatic repeat request, non-orthogonal multiple access, short-packet communications, intelligent reflecting surface, and Internet of Things.

Yalin Liu is a lecturer at the School of Science and Technology, Hong Kong Metropolitan University. She received her Ph.D. degree from Macau University of Science and Technology in 2022. From January 2022 to May 2022, she worked as a research assistant at the Education University of Hong Kong. Her research interests include Space-Air-Ground Integrated Networks, Web 3.0, Stochastic Geometry, Large-Scale Network Modeling, and Network Optimization. Dr. Liu has served as a Technical Program Committee (TPC) member for conferences such as IEEE WCNC and IEEE VTC, and as a reviewer for various IEEE journals including IEEE IoT and IEEE Communication Magazine. She is also serving as a Co-guest Editor for MDPI Electronics.

Kevin Hung (M'01-SM'19) received his Ph.D. in Electronic Engineering (concentration in biomedical engineering) from The Chinese University of Hong Kong (CUHK). He is currently an Associate Professor and the Head of the Department of Electronic Engineering and Computer Science in the School of Science and Technology, Hong Kong Metropolitan University (HKMU). His research interests include wearable technologies, mobile health, biological system modelling, quantum machine learning, and eye-tracking. He is currently serving as the Vice-chair of IEEE Hong Kong Section and Immediate Past Chair of the Electronics and Communications Section at IET Hong Kong.